Polyhedron 170 (2019) 388–394

Contents lists available at ScienceDirect

Polyhedron

journal homepage: www.elsevier.com/locate/poly

2,4,5-Triaryl imidazole probes for the selective chromo-fluorogenic detection of Cu(II). Prospective use of the Cu(II) complexes for the optical recognition of biothiols

Hazem Essam Okda [a,b,c], Sameh El Sayed [a,b,c], Ismael Otri [a,b,c], R. Cristina M. Ferreira [d], Susana P.G. Costa [d], M. Manuela M. Raposo [d,*], Ramón Martínez-Máñez [a,b,c,**], Félix Sancenón [a,b,c]

[a] Instituto Interuniversitario de Investigación de Reconocimiento Molecular y Desarrollo Tecnológico (IDM), Universitat Politècnica de València, Universitat de València, Spain
[b] Departamento de Química, Universitat Politècnica de València, Camino de Vera s/n, 46022 València, Spain
[c] CIBER de Bioingeniería, Biomateriales y Nanomedicina (CIBER-BBN), Spain
[d] Centro de Química, Universidade do Minho, Campus de Gualtar, 4710-057 Braga, Portugal

ARTICLE INFO

Article history:
Received 16 April 2019
Accepted 28 May 2019
Available online 13 June 2019

Keywords:
Imidazole-based probes
Cu(II) detection
Biothiols recognition
Cu(II) imaging
GSH imaging

ABSTRACT

The sensing behaviour toward metal cations and biothiols of two 2,4,5-triarylimidazole probes (**3a** and **3b**) is tested in acetonitrile and in acetonitrile–water. In acetonitrile the two probes present charge-transfer absorption bands in the 320–350 nm interval. Among all cations tested only Cu(II) is able to induce bathochromic shifts of the absorption band in the two probes, which is reflected in marked colour changes. Colour modulations are ascribed to the formation of 1:1 Cu(II)–probe complexes in which the cation interacts with the imidazole acceptor heterocycle. Besides, the two probes present intense emission bands (at 404 and 437 nm for **3a** and **3b** respectively) in acetonitrile that are quenched selectively by Cu(II). Probe **3a** is soluble in acetonitrile–water 1:1 (v/v) and Cu(II) also induces bathochromic shifts of the absorption bands. Moreover, the emission bands of probe **3a** in this mixed aqueous solutions is quenched in the presence of Cu(II). The potential use of the 1:1 complex formed between **3a** and Cu(II) for the chromo-fluorogenic detection of biothiols (GSH, Cys and Hcy) in aqueous environments is also tested. At this respect, addition of GSH, Cys and Hcy to acetonitrile–water 1:1 v/v solutions of **3a**–Cu(II) complex induces a hypsochromic shift of the visible band (reflected in a bleaching of the solutions) with a marked emission increase at 470 nm.

1. Introduction

In the last years, the development of chromo-fluorogenic chemosensors for transition metal cations has attracted the attention of researchers around the world [1]. These chromo-fluorogenic chemosensors are generally formed by two subunits, namely the binding site and the signalling group, that can be covalently linked or forming a supramolecular assembly [2]. In the first case, interaction of transition metal cations with the binding sites induces rearrangements in the π-conjugated system of the signalling unit which are reflected in colour and/or emission changes [3]. In the second approach, interaction of the transition metal cation with the binding site induces the displacement of the signalling unit from the initial complex to the solution [4].

Among transition metal cations, Cu(II) is one of the most abundant essential element in the human body and plays vital roles in several physiological processes. For instance, it has been reported that Cu(II) stimulates the proliferation of endothelial cells and is necessary for the secretion of several angiogenic factors by tumour cells [5,6]. Aside from its biological and environmental importance, copper is widely used in metallurgical, pharmaceutical and agrochemical industries [7]. As a result of the extensive applications of Cu(II) in life science and industry, it has become one of the first hazard environmental pollutants [8]. Despite the important role played by Cu(II) in several biological processes, abnormal levels of this cation can cause serious health problems on humans due to its ability to displace other vital metal ions in some enzyme-catalysed reactions [9]. In addition, high concentrations of Cu(II) in cells was documented to cause toxicity and different

* Corresponding author at: Centro de Química, Universidade do Minho, Braga, Portugal (M.M.M. Raposo).
** Corresponding author at: Instituto Interuniversitario de Investigación de Reconocimiento Molecular y Desarrollo Tecnológico (IDM), Universitat Politècnica de València, Universitat de València, Spain (R. Martínez-Máñez).
E-mail addresses: mfox@quimica.uminho.pt (M.M.M. Raposo), rmaez@ qim.upv.es (R. Martínez-Máñez).

https://doi.org/10.1016/j.poly.2019.05.055
0277-5387/

neurodegenerative diseases such as Menkes, Wilson's and Alzheimer [10]. Therefore, simple and rapid sensing tools to monitor Cu (II) levels in biological and environmental media are of importance. Besides, the World Health Organization (WHO) has recommended the maximum allowable level of Cu(II) in drinking water at 2.0 ppm (~30 μM) [11,12].

Currently, several complex analytical techniques are used to detect metal ions such as electrochemical measurements, atomic absorption spectrometry and inductively coupled plasma mass spectroscopy [13,14]. However, these techniques are time-consuming, needs sample pre-treatment, used expensive equipment's, required trained personnel and cannot be used *in situ*.

On the other hand, biothiols (such as the amino acids cysteine (Cys) and homocysteine (Hcy) and the tripeptide glutathione (GSH)) play vital roles in cellular processes related with the damage of cellular components by reactive oxygen species (ROS) [15,16]. Levels of biothiols in cells are controlled by the equilibrium between thiols and disulfides. Besides, the relative levels of biothiols can be used as biomarkers for aging, neurodegenerative pathologies and many other diseases such as cancer, AIDS and cystic fibrosis among others [17,18]. Thus, taking into account the above mentioned facts, determination of biothiols especially in biological samples is an important issue. Actually, different analytical methods are available to determination of biothiol levels including HPLC, capillary electrophoresis, and mass spectrometry [19–21]. As an alternative to these classical techniques, in the past two decades, a number of chromo-fluorogenic probes for biothiol detection have been reported [22–24]. Most of the described examples are based on the chemodosimeter approach and are synthesized taking into account the nucleophilic character of thiol moieties in these biomolecules [25–31]. Also, the displacement approach has been extensively used to design biothiol selective chromo-fluorogenic probes. For this purpose, the emission quenching features of transition metal ions such as Cu(II) has been widely used. The basis of these probes is the generation of non-emissive Cu(II) complexes with fluorophores equipped with coordinating subunits. In the presence of biothiols, there is a demetallation process, restoring the full emission of the fluorophore [32–37]. However, many of the described biothiols chemosensors did not work in pure water or in mixed aqueous environments. Besides, the selectivity achieved in most cases is low because probes are unable to distinguish between Cys, Hcy and GSH. In fact, the synthesis and characterization of probes for the selective recognition of individual biothiol in aqueous environments is of interest.

Taking into account our interest in the development of chromo-fluorogenic probes for biomolecules [38–45] we report herein the synthesis, characterization and binding studies toward Cu(II) and biothiols (GSH, Hcy and Cys), of two probes containing 2,4,5-trisubstitued imidazole moieties (**3a** and **3b** in Scheme 1). The prepared probes contain electron donor (furan) and electron acceptor (phenanthroline) rings of different strength covalently linked with an imidazole heterocycle. 2,4,5-triaryl(heteroaryl)-imidazole based chromophores have received increasing attention due to their distinctive optical properties, applications in medicinal chemistry and materials sciences, and as nonlinear optical materials (SHG chromophores, two-photon absorbing molecules) and thermally stable luminescent materials for several applications (such as OLEDs and fluorescent probes).

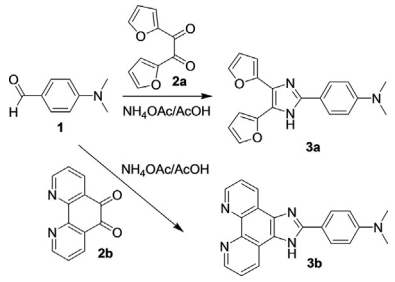

Scheme 1. One pot synthesis of imidazole probes **3a** and **3b**.

2. Experimental

2.1. Materials and methods

All melting points were measured on a Stuart SMP3 melting point apparatus. TLC analyses were carried out on 0.25 mm thick pre-coated silica plates (Merck Fertigplatten Kieselgel 60F_{254}) and spots were visualised under UV light. Chromatography on silica gel was carried out on Merck Kieselgel (230–240 mesh). IR spectra were determined on a BOMEM MB 104 spectrophotometer using KBr discs. NMR spectra were obtained on a Bruker Avance III 400 at an operating frequency of 400 MHz for ^{1}H and 100.6 MHz for ^{13}C using the solvent peak as internal reference at 25 °C. All chemical shifts are given in ppm using $^\delta$H Me_4Si = 0 ppm as reference. Assignments were supported by spin decoupling-double resonance and bidimensional heteronuclear correlation techniques. UV–Vis titration profiles were carried out with JASCO V-650 spectrophotometer (Easton, MD, USA). Fluorescence measurements were recorded with a JASCO FP-8500 spectrophotometer. Commercially available reagents 4-(dimethylamino)benzaldehyde (**1**), 1,2-di(furan-2-yl)ethane-1,2-dione (**2a**), 1,10-phenanthroline-5,6-dione (**2b**) and ammonium acetate were purchased from Sigma-Aldrich and Acros and used as received.

2.1.1. Synthesis of 4-(4,5-di(furan-2-yl)-1H-imidazol-2-yl)-N,N-dimethylbenzenamine (**3a**)

4-(Dimethylamino)benzaldehyde (**1**, 0.15 g, 1 mmol), 1,2-di(furan-2-yl)ethane-1,2-dione (**2a**, 0.19 g, 1 mmol) and NH_4OAc (1.54 g, 20 mmol) were dissolved in glacial acetic acid (5 mL), followed by stirring and heating at reflux for 8 h. The reaction mixture was then cooled to room temperature, ethyl acetate was added (15 mL) and the mixture was washed with water (3 × 10 mL). After drying the organic phase with anhydrous $MgSO_4$, the solution was filtered and the solvent was evaporated to dryness. The resulting crude product was purified by column chromatography (silica gel, DCM/MeOH 100:1 v/v); yield (64 mg, 60%) as grey solid. Mp = 240.2–240.9 °C.

^{1}H NMR (400 MHz, DMSO-d_6): δ = 2.95 (s, 6H), 6.55 (s, 1H), 6.63 (br s, 1H), 6.71 (d, J = 2.0 Hz, 1H), 6.77 (dd, J = 8.8 and 2.0 Hz, 2H), 6.89 (d, J = 2.8 Hz, 1H), 7.68 (br s, 1H), 7.78 (br s, 1H), 7.90 (dd, J = 8.8 and 2.0 Hz, 2H), 12.47 (s, 1H, NH) ppm. ^{13}C NMR (100.6 MHz, DMSO-d_6): δ = 39.89, 106.56, 107.81, 111.33, 111.80, 117.50, 118.27, 126.68, 129.15, 141.61, 142.22, 144.79, 147.23, 149.59, 150.53 ppm. IR (Nujol): ν = 3570, 1665, 1612, 1530, 1494, 1222, 1202, 1169, 1122, 1074, 1014, 986, 943, 911, 885, 815 cm^{-1}. HRMS-EI m/z: calcd for $C_{19}H_{17}N_3O_2$+H$^+$: 320.1399; measured: 320.1394.

2.1.2. Synthesis of 4-(1H-imidazo[4,5-f][1,10]phenanthrolin-2-yl)-N,N-dimethylbenzenamine (3b)

4-(Dimethylamino)benzaldehyde (**1**, 0.15 g, 1 mmol), 1,10-phenanthroline-5,6-dione (**2b**, 0.2 g, 1 mmol) and NH_4OAc (1.54 g, 20 mmol) were dissolved in glacial acetic acid (5 mL), followed by stirring and heating at reflux for 8 h. The reaction mixture was then cooled to room temperature, ethyl acetate was added (15 mL) and the mixture was washed with water (3 × 10 mL). After drying the organic phase with anhydrous $MgSO_4$, the solution was filtered and the solvent was evaporated

to dryness. The resulting crude product was purified by column chromatography (silica gel, DCM/MeOH 98:2 v/v); yield (8 mg, 7%) as yellow oil.

^{1}H NMR (400 MHz, DMSO-d_6): δ = 3.02 (s, 6H), 6.90 (d, J = 9.2 Hz, 2H), 7.81–7.84 (m, 2H,), 8.11 (dd, J = 8.8 and 2.0 Hz, 2H), 8.92 (dd, J = 8.0 and 1.6 Hz, 2H), 9.00 (dd, J = 4.0 and 2.0 Hz, 2H), 13.40 (s, 1H, NH) ppm. ^{13}C NMR (100.6 MHz, DMSO-d_6): δ = 40.13, 111.97, 117.29, 123.33, 127.45, 127.62, 129.77, 142.94, 147.34, 147.40, 151.21, 151.88 ppm. IR (liquid film): ν = 3414, 2925, 1657, 1611, 1502, 1438, 1372, 1351, 1195, 1168, 1125, 1067, 1024, 946, 814, 739 cm^{-1}. HRMS-EI m/z: calcd for $C_{21}H_{17}N_5$+H$^+$: 340.1562; measured: 340.1560.

2.2. UV–Vis and emission measurements

Stock solutions of the cations (i.e., Cu(II), Pb(II), Mg(II), Ge(II), Ca(II), Zn(II), Co(II), Ni(II), Ba(II), Cd(II), Hg(II), Fe(III), In(III), As(III), Al(III), Cr(III), Ga(III), K(I), Li(I) and Na(I) as perchlorate salts) were prepared at (1.0×10^{-3} mol L^{-1}) in acetonitrile. The concentrations of probes used in spectroscopy measurements were ca. (5.0×10^{-5} mol L^{-1}) and (1.0×10^{-5} mol L^{-1}). We took care that the maximum addition of cations solutions did not exceed 10% of the volume of the receptor to avoid significant changes in the total solution concentration. In the experiments that required the addition of excess of ions (20 equiv.), corrections of the volume and concentration were made. The UV–Vis and fluorometric titrations were carried out at room temperature (25 °C).

3. Results and discussion

3.1. Synthesis and characterization of probes **3a-b**

Heteroaromatic commercially available diones **2a** and **2b** containing furyl and phenanthroline rings (see Scheme 1) were used as precursors for the synthesis of **3a** and **3b**. The synthesis of probes **3a** and **3b** was previously described [45,46]. The final probes were prepared through a condensation reaction between diones **2a** and **2b** and 4-(*N*,*N*-dimethylamino)benzaldehyde (**1**) in presence of ammonium acetate and glacial acetic acid at reflux under Debus-Radziszewski imidazole synthesis conditions (see also Scheme 1) [47]. Probes were synthesized in fair to moderate yields (Table 1) as a consequence of several factors such as the difficulty in the purification step due to the polarity of the compounds as well as their decomposition during the long reaction times under hard conditions (acetic acid reflux). The final probes **3a** and **3b** were completely characterized by ^{1}H and ^{13}C NMR, IR, and mass spectrometry. The data obtained are in full agreement with the proposed formulations (see Section 2).

One of the most characteristic ^{1}H NMR signals of probes **3a** and **3b** is that corresponding to the N—H proton in the imidazole ring (see Table 1). As could be seen, a clear correlation between the electronic nature of the rings (furan and phenanthroline) directly linked with imidazole and the shift of the N—H proton of this heterocycle was observed. At this respect, probe **3b** bearing the electron deficient phenanthroline system exhibited the highest chemical shift for the nitrogen proton of the imidazole ring (13.40 ppm). On the other hand, probe **3a** functionalized with electron rich furan heterocycle exhibit lower chemical shifts for the nitrogen proton of the imidazole ring (12.45 ppm) when compared to **3b**.

Table 1
Yields and ^{1}H NMR data of imidazole probes **3a** and **3b** at 400 MHz in DMSO-d_6.

Probe	Yield (%)	δ_H NH (ppm)
3a	60	12.45
3b	7	13.40

3.2. UV–Vis and emission spectroscopic behaviour of probes **3a-b** in the presence of selected metal cations in acetonitrile

In a first step, UV–Vis changes of both probes in acetonitrile were studied. Acetonitrile solutions of **3a** and **3b** (1.0×10^{-5} mol L^{-1}) showed intense absorption bands in the UV zone (321 nm for **3a** and 341 nm for **3b**). The observed absorption bands are ascribed to charge-transfer transitions between the *N*,*N*-dimethylamino donor moiety and imidazole acceptor heterocycle. Besides, the wavelength of the charge-transfer band was affected by the aromatic units directly connected with the central imidazole heterocycle. At this respect, the presence of electron deficient phenanthroline unit in probe **3b** induced the larger charge-transfer character and the associated absorption appeared at the higher wavelength (341 nm). On the other hand, in probe **3a**, the imidazole core was linked to an electron donating heterocycle (furan) and, as a consequence, absorption bands are shifted to lower wavelengths (321 nm).

Besides, both probes were highly emissive in acetonitrile upon excitation at the maximum of the absorbance of the visible band. At this respect, excitation at 321 nm of acetonitrile solutions of probe **3a** (1.0×10^{-5} mol L^{-1}) induced the appearance of a marked emission band centred at 404 nm. Nearly the same results were obtained for probe **3b** with an intense emission centred at 437 nm. Besides, the quantum yield of the two probes (determined using pyrene as standard, see Supporting Information for details) was 0.41 and 0.31 for **3a** and **3b** respectively.

Then, UV–Vis changes in acetonitrile solutions of both probes (1.0×10^{-5} mol L^{-1}) in the presence of increasing amounts (from 0.1 to 10 eq.) of selected metal cations (Cu(II), Pb(II), Mg(II), Ge(II), Ca(II), Zn(II), Co(II), Ni(II), Ba(II), Cd(II), Hg(II), Fe(III), In(III), As(III), Al(III), Cr(III), Ga(III), K(I), Li(I) and Na(I)) were tested. The two probes showed nearly the same behaviour and in all cases only Cu(II) induced the progressive appearance of a new redshifted absorption band. Fig. 1 shows the set of spectra obtained upon addition of increasing quantities of Cu(II) cation to an acetonitrile solution of probe **3a**. As could be seen in Fig. 1, addition of Cu(II) induced a progressive bathochromic shift together with a marked decrease of the band centred at 321 nm with the concomitant

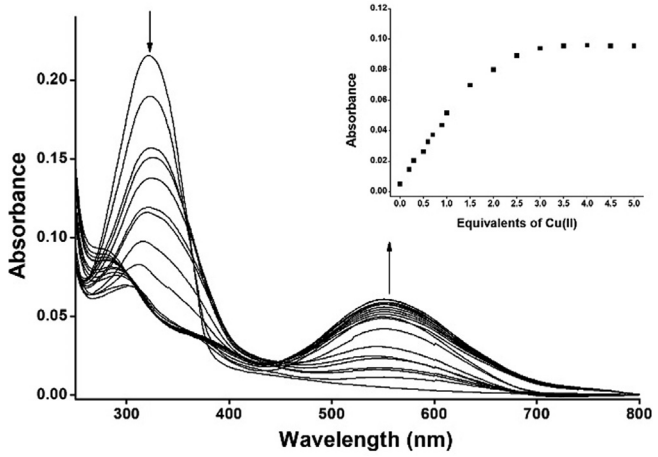

Fig. 1. UV–Vis titration profile of probe **3a** in acetonitrile (1.0×10^{-5} mol L^{-1}) upon addition of increasing quantities of Cu(II) cation (0–10 eq.). Inset: Absorbance at 563 nm vs equivalents of Cu(II) added.

appearance of a redshifted absorption at 563 nm. Besides, a marked colour change from colourless to violet was observed.

Nearly the same behaviour was observed with probe **3b** in the presence of Cu(II) cation. Addition of Cu(II) to an acetonitrile solution of **3b** induced the appearance of a new absorbance at 466 nm with a marked colour change from colourless to yellow. Changes upon addition of Cu(II) to acetonitrile solutions of **3a** and **3b** was ascribed to the formation of complexes in which the cation interacts with the acceptor part of the probes (i.e. the imidazole heterocycle).

In a next step, the emission of probes **3a** and **3b** in acetonitrile (1.0×10^{-5} mol L^{-1}) was also studied upon addition of increasing amounts of selected cations. A marked selective response was obtained for Cu(II) that was the unique cation able to induce a remarkable emission quenching for both probes. Fig. 2 shows the set of emission spectra obtained upon addition of increasing amounts of Cu(II) to probe **3a**. Addition of Cu(II) induced a progressive quenching of the emission band of **3a** at 404 nm (excitation at ca. 380 nm) together with a hypsochromic shift of ca. 10 nm. A similar quenching and hypsochromic shifts of the emission bands was observed upon addition of Cu(II) to acetonitrile solutions of probe **3b** (see Supporting Information). The obtained results are in accordance with the marked and well-known quenching behaviour of Cu(II) cation.

From the UV–Vis and emission titration profiles obtained for both probes, the limits of detection (LOD) for Cu(II) in acetonitrile were determined (see Table 2). LODs were assessed using the 3.3* (σ/s) equation, where σ is the standard error of the predicted Y-value vs. each X (i.e. Cu(II) concentration), and s is the slope for the linear relationship. Both probes presented similar Cu(II) LODs in the 0.9–2.0 μM range.

3.3. Determination of binding stoichiometries and stability constants of probe *3a* and *3b* with Cu(II) in acetonitrile

In order to complete the characterization of the complex formed between probe **3a** and **3b** and Cu(II) cation we carried out UV–Vis and emission studies to obtain Job's plots to assess the binding stoichiometry and to determine the stability constants.

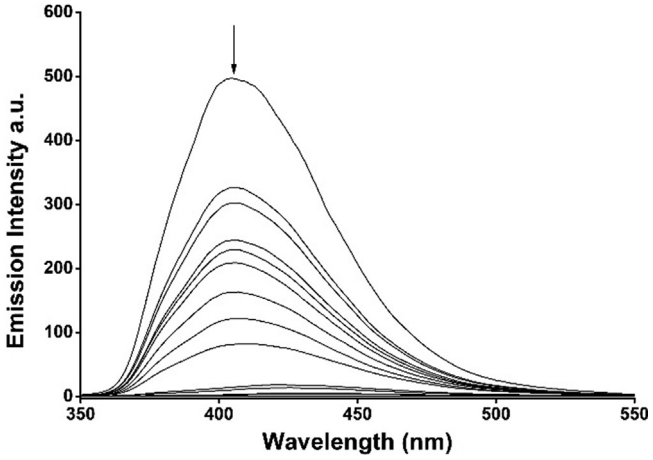

Fig. 2. Fluorescence titration profile of probe **3a** in acetonitrile (1.0×10^{-5} mol L^{-1}) upon addition of increasing quantities of Cu(II) cation (0–10 equiv.).

Table 2
Limits of detection of Cu(II) measured for **3a** and **3b** probes in acetonitrile.

Probe	UV–Vis [μM]	Emission [μM]
3a	0.9	1.0
3b	1.2	2.0

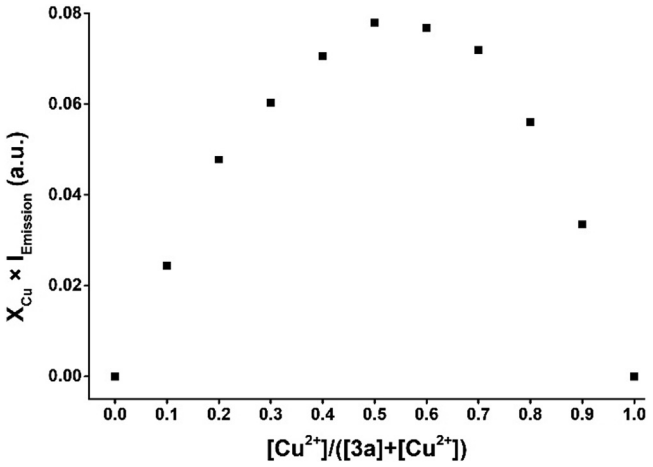

Fig. 3. Job's plot for the binding of **3a** with Cu(II). Absorbance at 555 nm was plotted as a function of the molar ratio [Cu(II)]/([**3a**] + [Cu(II)]). The total concentration of Cu(II) and probe **3a** was (2.0×10^{-5} mol L^{-1}).

Job's plots, constructed using UV–Vis measurements in acetonitrile, showed that **3a** and **3b** formed 1:1 complexes with Cu(II). As an example, Fig. 3 showed the Job's plot obtained for probe **3a**. Besides, from the UV–Vis and fluorescence titration profiles obtained for probes **3a** and **3b** in the presence of Cu(II) cation, the stability constant for the formation of the corresponding 1:1 complexes were determined. The obtained values are shown in Table 3.

3.4. UV–Vis and emission spectroscopic behaviour of probes *3a* and *3b* in the presence of selected metal cations in aqueous environments

In order to assess the possible use of both probes for Cu(II) detection in real samples, the UV–Vis and emission response toward Cu(II) was tested in aqueous environments. Probes **3a** and **3b** were fully solubilized in water (pH 7.4)–acetonitrile 1:1 v/v. In this medium, both probes showed charge-transfer absorption bands centred at 321 and 339 nm for **3a** and **3b** respectively. The maxima of the charge-transfer band in water–acetonitrile 1:1 v/v were very similar to those measured in pure acetonitrile, indicating that conformation and hydration of the probes did not change, to any remarkable extent, the energy of their electronic levels in the basal state.

Next, the UV–Vis behaviour of aqueous solutions of both probes (5.0×10^{-5} mol L^{-1}) in the presence of selected metal cations was tested. None of the metal cations tested induced changes in the absorption bands of probe **3b**. In contrast, for probe **3a**, only Cu (II) induced the appearance of a new redshifted absorption at 563 nm as could be seen in Fig. 4 (similar to that found in acetonitrile) together with marked colour changes (Fig. 5).

More in detail, addition of increasing quantities of Cu(II) cation to water (pH 7.4)–acetonitrile 1:1 v/v (5.0×10^{-5} mol L^{-1})

Table 3
Logarithms of binding constants measured for the interaction of probes **3a** and **3b** with Cu(II) in acetonitrile.

Probe	Log *K*	
	UV–Vis	Emission
3a	5.1 ± 0.1	6.4 ± 0.3
3b	5.8 ± 0.9	5.8 ± 0.1

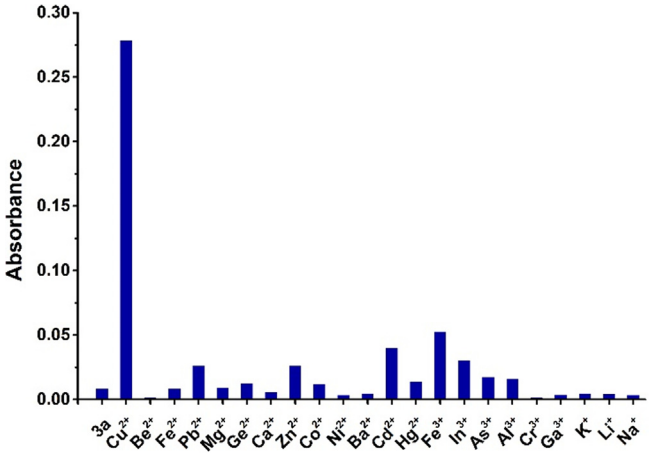

Fig. 4. Absorption of probe **3a** at 563 nm (water (pH 7.4)–acetonitrile 1:1 v/v, 5.0×10^{-5} mol L^{-1}) in the presence of 10 eq. of selected metal cations.

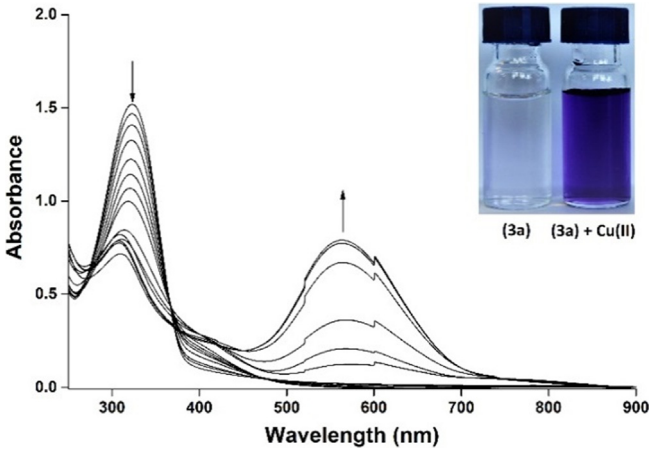

Fig. 5. UV–Vis titration profile of probe **3a** in water (pH 7.4)–acetonitrile 1:1 v/v (5.0×10^{-5} mol L^{-1}) upon addition of increasing quantities of Cu(II) cation (0–10 eq.). Inset: colour change when Cu(II) cation was added to water (pH 7.4)–acetonitrile 1:1 v/v solutions of probe **3a**.

solutions of probe **3a** induced a moderate decrease of the absorption at 321 nm and the simultaneous appearance of a new band centred at 563 nm (see Fig. 5). These spectral changes were reflected in a clear colour change from colourless to violet (see inset in Fig. 5). Besides, from the titration profile at 489 nm, a limit of detection for Cu(II) of 2.60 μM was determined.

On the other hand, **3a** was highly emissive in water (pH 7.4)–acetonitrile 1:1 v/v solutions showing a remarkable emission band at 420 nm (excitation at 321 nm). Moreover, fluorescence changes in the presence of selected metal cations was tested. For this purpose, solutions of probe **3a** were excited at the isosbestic point observed in the UV–Vis titration profile (ca. 375 nm) and the emission recorded after the addition of different amounts of selected cations. From all cations tested, only Cu(II) was able to induce a response which consisted of a marked emission quenching of the emission band 420 nm (see Fig. 6). The obtained results clearly resemble those obtained for probe **3a** in acetonitrile in the presence of Cu(II) cation. From the emission titration profile (see also Fig. 6), a LOD for Cu(II) of 3.4 μM for **3a** was determined. This LOD is higher than that found in acetonitrile, most likely as consequence of a stronger solvation of Cu(II) cation in water.

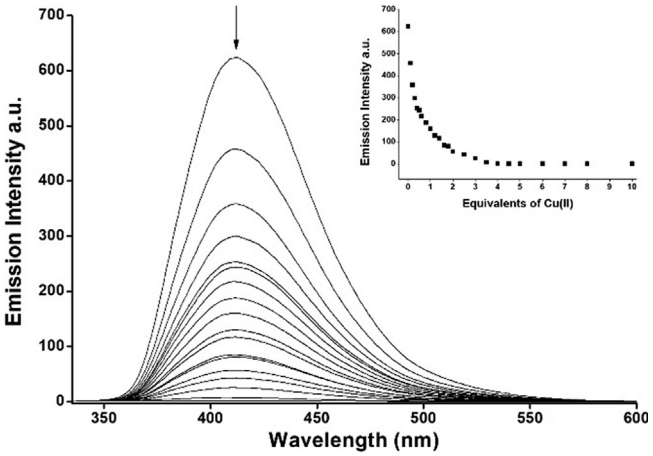

Fig. 6. Fluorescence titration profile of probe **3a** in water (pH 7.4)–acetonitrile 1:1 v/v (5.0×10^{-5} mol L^{-1}) upon addition of increasing amounts of Cu(II) cation (from 0 to 10 eq.). Inset: Emission intensity at 420 nm vs equivalents of Cu(II) added.

3.5. Spectroscopic detection of biothiols

In this section we studied the potential use of the **3a**·Cu complex for the recognition of biothiols [48]. Studies were carried out in the presence of selected amino acids (Ala, Arg, Asp, Cys, Gln, Glu, Gly, Hcy, His, Ile, Leu, Lys, Met, Phe, Pro, Ser, Thr, Trp, Tyr and Val) and small peptides (GSH).

Water (pH 7.4)–acetonitrile 1:1 v/v solution of complex **3a**·Cu (6.2×10^{-6} mol L^{-1}, formed *in situ* by the addition of equimolar quantities of probe and Cu(II) cation) shows an intense absorption band at 563 nm which was the responsible of the strong violet colour observed. From all amino acids (0.2 eq.) and peptides (0.2 eq.) tested, only in the presence of thiol-containing molecules (Cys, Hcy and GSH) a bleaching of the solution was observed (see Fig. 7). Besides, water (pH 7.4)–acetonitrile 1:1 v/v solutions of the **3a**·Cu complex (6.2×10^{-6} mol L^{-1}) were weakly emissive and only addition of Cys, Hcy and GSH induced a marked emission enhancement at 420 nm (see Fig. 8). The chromo-fluorogenic changes observed upon addition of biothiols to the aqueous solutions of **3a**·Cu complex are ascribed to a demetallation of the complex, that released the free probe **3a**. Finally, from UV–Vis and fluorescence titration

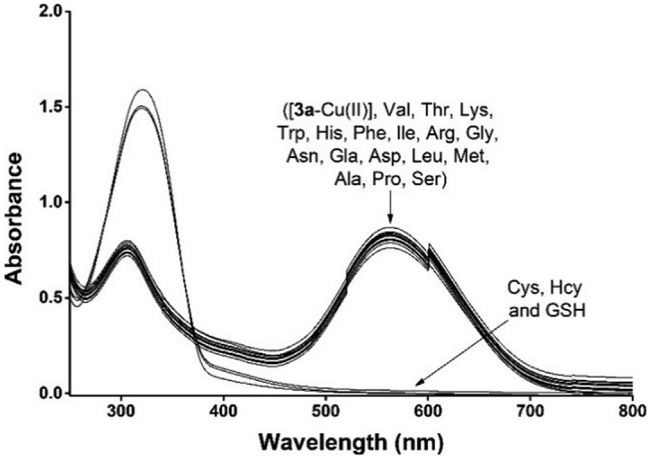

Fig. 7. UV–Vis changes of **3a**·Cu (6.2×10^{-6} mol L^{-1}) in water (pH 7.4)–acetonitrile 1:1 v/v in the presence of selected amino acids (0.2 eq.) and biothiols (0.2 eq.).

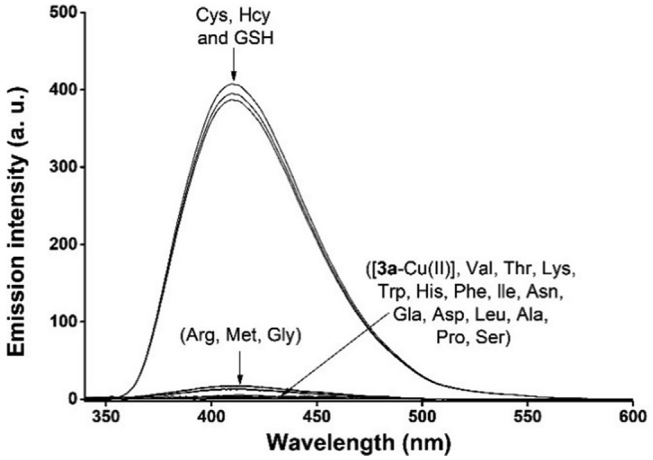

Fig. 8. Changes in the emission band of **3a**·Cu complex (6.2×10^{-6} mol L^{-1}) in water (pH 7.4)–acetonitrile 1:1 v/v upon addition of biothiols (0.2 eq.) and selected amino acids (0.2 eq.).

Table 4
Limits of detection of biothiols measured for **3a**·Cu in aqueous solutions.

Complex	UV–Vis (μM)			Fluorescence (μM)		
	GSH	Cys	Hcy	GSH	Cys	Hcy
3a·Cu	0.6	1.3	0.8	0.6	0.9	0.7

profiles obtained for **3a**·Cu, the LODs for biothiols were determined (Table 4).

4. Conclusions

In summary, we show herein the synthesis and chromo-fluorogenic behaviour toward metal cations and biothiols of easy to prepare imidazole-containing probes **3a** and **3b**. Acetonitrile solutions of both probes were characterized by the presence of a charge-transfer absorption band in the 320–350 range. Both probes were moderately emissive in acetonitrile. From all cations tested only Cu(II) induced the growth of new redshifted bands in the 450–570 nm interval. Besides, the emission bands of both receptors were quenched in the presence of Cu(II) cation. These spectral changes were ascribed to a preferential coordination of Cu(II) cation with the electron acceptor imidazole heterocycle. Only probe **3a** changed its UV–Vis and emission spectra in the presence of Cu(II) in water–acetonitrile mixtures. On the other hand, weakly emissive complex **3a**·Cu was used to detect biothiols (GSH, Cys and Hcy) in water–acetonitrile 1:1 v/v solution. In the presence of biothiols, the visible bands of the complex disappeared and the emission intensity of the free probe was fully restored. These changes were ascribed to a demetallation process.

Acknowledgments

We thank the Spanish Government (MAT2015-64139-C4-1-R) and Generalitat Valenciana (PROMETEO 2018/024). H. E. O. thanks Generalitat Valenciana for his Grisolia fellowship. Thanks are also due to Fundação para a Ciência e Tecnologia (Portugal) for financial support to the Portuguese NMR network (PTNMR, Bruker Avance III 400-Univ. Minho), FCT and FEDER (European Fund for Regional Development)-COMPETEQREN-EU for financial support to the research centre CQ/UM [Ref. UID/QUI/00686/2013 and UID/ QUI/0686/2016], and a PhD grant to R. C. M. Ferreira (SFRH/BD/86408/2012).

Appendix A. Supplementary data

Supplementary data to this article can be found online at https://doi.org/10.1016/j.poly.2019.05.055.

References

[1] D. Udhayakumari, S. Naha, S. Velmathi, Anal. Methods 9 (2017) 552.
[2] J. Wu, B. Kwon, W. Liu, E.V. Anslyn, P. Wang, J.S. Kim, Chem. Rev. 115 (2015) 7893.
[3] J. Zhang, F. Cheng, J. Li, J.J. Zhu, Y. Lu, Nano Today 11 (2016) 309.
[4] J. Cheng, X. Zhou, H. Xiang, Analyst 140 (2015) 7082.
[5] S. Swaminathan, P. Gangadaran, T. Venkatesh, M. Ghosh, J. Pharm. Biomed. Sci. 9 (2011) 1.
[6] S. Kamble, B. Utage, P. Mogle, R. Kamble, S. Hese, B. Dawane, R. Gacche, AAPS Pharm. Sci. Technol. 17 (2016) 1030.
[7] A.K. Jain, R.K. Singh, S. Jain, J. Raisoni, Transition Met. Chem. 33 (2008) 243.
[8] S. Goswami, D. Sen, N.K. Das, G. Hazra, Tetrahedron Lett. 51 (2010) 5563.
[9] Q. Xie, T. Zhou, L. Yen, M. Shariff, T. Nguyen, K. Kami, P. Gu, L. Liang, J. Rao, R. Shi, Nutr. Diet. Suppl. 5 (2013) 1.
[10] X.Y. Choo, L. Alukaidey, A.R. White, A. Grubman, Int. J. Alzheimer's Dis. 2013 (2013) 145345.
[11] B. Sarkar, Chem. Rev. 99 (1999) 2535.
[12] K.J. Barnham, C.L. Masters, A.I. Bush, Nat. Rev. Drug Discov. 3 (2004) 205.
[13] C.M. Ackerman, S. Lee, C.J. Chang, Anal. Chem. 89 (2017) 22.
[14] H. Hotta, K. Tsunoda, Anal. Sci. 31 (2015) 7.
[15] D.M. Townsend, K.D. Tew, H. Tapiero, Biomed. Pharmacother. 57 (145–15) (2003) 5.
[16] J.W. Miller, S.A. Beresford, M.L. Neuhouser, T.Y. Cheng, X. Song, E.C. Brown, Y. Zheng, B. Rodriguez, R. Green, C.M. Ulrich, Am. J. Clin. Nutr. 97 (2013) 827.
[17] J. Dorszewska, M. Prendecki, A. Oczkowska, M. Dezor, W. Kozubski, Curr. Alzheimer Res. 13 (2016) 952.
[18] A. Rozycka, P.P. Jagodzinski, W. Kozubski, M. Lianeri, J. Dorszewska, Curr. Genomics 14 (2013) 534.
[19] T. Santa, Drug Discovery Ther. 7 (2013) 172.
[20] F. Carlucci, A. Tabucchi, J. Chromatogr. B: Analyt. Technol. Biomed. Life Sci. 877 (2009) 3347.
[21] I.A. Blair, Biomed. Chromatogr. 24 (2010) 29.
[22] M. Isik, T. Ozdemir, I.S. Turan, S. Kolemen, E.U. Akkaya, Org. Lett. 15 (2013) 216.
[23] Y.C. Liao, P. Venkatesan, L.F. Wei, S.P. Wu, Sens. Actuators, B Chem. 232 (2016) 732.
[24] K.S. Lee, J. Park, H.J. Park, Y.K. Chung, S.B. Park, H.J. Kim, I.S. Shin, J.I. Hong, Sens. Actuators B Chem. 237 (2016) 256.
[25] F. Kong, R. Liu, R. Chu, X. Wang, K. Xu, B. Tang, Chem. Commun. 49 (2013) 9176.
[26] J. Zhang, X.D. Jiang, X. Shao, J. Zhao, Y. Su, D. Xi, H. Yu, S. Yue, L.J. Xiao, W. Zhao, RSC Adv. 4 (2014) 54080.
[27] Y.W. Wang, S.B. Liu, W.J. Ling, Y. Peng, Chem. Commun. 52 (2016) 827.
[28] J. Liu, Y.Q. Sun, H. Zhang, Y. Huo, Y. Shi, W. Guo, Chem. Sci. 5 (2014) 3183.
[29] Y.S. Guan, L.Y. Niu, Y.Z. Chen, L.Z. Wu, C.H. Tung, Q.Z. Yang, RSC Adv. 4 (2014) 8360.
[30] Z.H. Fu, X. Han, Y. Shao, J. Fang, Z.H. Zhang, Y.W. Wang, Y. Peng, Anal. Chem. 89 (2017) 1937.
[31] Y.L. Yang, F.M. Zhang, Y.W. Wang, B.X. Zhang, R. Fang, J.G. Fang, Y. Peng, Chem. Asian J. 10 (2015) 422.
[32] Z.H. Fu, L.B. Yan, X. Zhang, F.F. Zhu, X.L. Han, J. Fang, Y.W. Wang, Y. Peng, Org. Biomol. Chem. 15 (2017) 4115.
[33] Y. Singh, S. Arun, B.K. Singh, P.K. Dutta, T. Ghosh, RSC Adv. 6 (2016) 80268.
[34] S.H. Lee, J.J. Lee, J.W. Shin, K.S. Min, C. Kim, Dyes Pigm. 116 (2015) 131.
[35] D. Maheshwaran, T. Nagendraraj, P. Manimaran, B. Ashokkumar, M. Kumar, R. Mayilmurugan, Eur. J. Inorg. Chem. (2017) 1007.
[36] Y.S. Kim, G.J. Park, S.A. Lee, C. Kim, RSC Adv. 5 (2015) 31179.
[37] G.R. You, J.J. Lee, Y.W. Choi, S.Y. Lee, C. Kim, Tetrahedron 72 (2016) 875.
[38] L.E. Santos-Figueroa, A. Llopis-Lorente, S. Royo, F. Sancenón, R. Martínez-Máñez, A.M. Costero, S. Gil, M. Parra, ChemPlusChem 80 (2015) 800.
[39] C. Marín-Hernández, L.E. Santos-Figueroa, S. El Sayed, T. Pardo, M.M.M. Raposo, R.M.F. Batista, S.P.G. Costa, F. Sancenón, R. Martínez-Máñez, Dyes Pigm. 122 (2015) 50.
[40] M. Lo Presti, S. El Sayed, R. Martínez-Máñez, A.M. Costero, S. Gil, M. Parra, F. Sancenón, New J. Chem. 40 (2016) 9042.
[41] S. El Sayed, C. de la Torre, L.E. Santos-Figueroa, E. Pérez-Paya, R. Martínez-Máñez, F. Sancenón, A.M. Costero, M. Parra, S. Gil, RSC Adv. 3 (2013) 25690.
[42] S. El Sayed, C. de la Torre, L.E. Santos-Figueroa, R. Martínez-Máñez, F. Sancenón, Supramol. Chem. 4 (2015) 244.
[43] C. Marín-Hernández, L.E. Santos-Figueroa, M.E. Moragues, M.M.M. Raposo, R. M.F. Batista, S.P.G. Costa, T. Pardo, R. Martínez-Máñez, F. Sancenón, J. Org. Chem. 79 (2014) 10752.

[44] H.E. Okda, S. El Sayed, I. Otri, R.C.M. Ferreira, S.P.G. Costa, M.M.M. Raposo, R. Martínez-Máñez, F. Sancenón, Dyes Pigm. 162 (2019) 303.
[45] K. Nakashima, Y. Fukuzaki, R. Nomura, R. Shimoda, Y. Nakamura, N. Kuroda, S. Akiyama, K. Irgum, Dyes Pigm. 38 (1998) 127.
[46] Z.Q. Bian, K.Z. Wang, L.P. Jin, Polyhedron 21 (2002) 313.
[47] H.E. Okda, S. El Sayed, R.C.M. Ferreira, S.P.G. Costa, M.M.M. Raposo, R. Martínez-Máñez, F. Sancenón, Dyes Pigm. 159 (2018) 45.
[48] S. Mandal, G. Das, R. Singh, R. Shukla, P.K. Bharadwaj, Coord. Chem. Rev. 160 (1997) 191.